Environ. Sci. Technol. **2001**, *35,* 3433−3441

Distribution and Retention of ^{137}Cs in Sediments at the Hanford Site, Washington

JAMES P. MCKINLEY,*,† CYNTHIA J. ZEISSLER,‡ JOHN M. ZACHARA,† R. JEFFREY SERNE,† RICHARD M. LINDSTROM,‡ HERBERT T. SCHAEF,† AND ROBERT D. ORR†

Pacific Northwest National Laboratory, Richland, Washington 99352, and National Institute for Standards and Technology, 100 Bureau Drive, Gaithersburg, Maryland 20899-8371

$^{137}Cesium$ and other contaminants have leaked from single-shell storage tanks (SSTs) into coarse-textured, relatively unweathered unconsolidated sediments. Contaminated sediments were retrieved from beneath a leaky SST to investigate the distribution of adsorbed $^{137}Cs^+$ across different sediment size fractions. All fractions contained mica (biotite, muscovite, vermiculatized biotite), quartz, and plagioclase along with smectite and kaolinite in the clay-size fraction. A phosphor-plate autoradiograph method was used to identify particular sediment particles responsible for retaining $^{137}Cs^+$. The Cs-bearing particles were found to be individual mica flakes or agglomerated smectite, mica, quartz, and plagioclase. Of these, only the micaceous component was capable of sorbing Cs^+ strongly. Sorbed $^{137}Cs^+$ could not be significantly removed from sediments by leaching with dithionite citrate buffer or KOH, but a fraction of the sorbed $^{137}Cs^+$ (5−22%) was desorbable with solutions containing an excess of Rb^+. The small amount of $^{137}Cs^+$ that might be mobilized by migrating fluids in the future would likely sorb to nearby micaceous clasts in downgradient sediments.

Introduction

The Hanford Site in eastern Washington is the subject of a vast remediation effort. Approximately 40 yr of Pu production created large volumes of waste, some of which reside in sediments as environmental contaminants. ^{137}Cs was a major component of the radioactive wastes. The chemical controls on the mobility of this nuclide and the strength with which it is bound in the subsurface have bearing on remediation activities at the site.

Much low-level waste was dumped directly to ground at the site, and most of the high-level waste was stored in 162 massive underground tanks, ranging in capacity from 210 to 4100 m^3 (55 000−1.1 million gal). The chemically complex wastes had variable composition because at least six different reprocessing schemes were used to extract Pu and recover other elements such as U. A common feature was a high concentration of $NaNO_3/NO_2$ salts (>0.5 mol/L). Approximately 40% of the tanks' total radioactivity originated from ^{137}Cs, which is highly soluble and found in the liquid supernate at activities ranging up to 2×10^{10} Bq/L (0.5 Ci/L = 0.000 041 mol ^{137}Cs/L), with many tanks falling in the range of 0.4−1.5 $\times 10^{10}$ Bq/L.

Sixty-seven of the tanks are known to have leaked, discharging over 3800 m^3 (>1 million gal) of supernate and approximately 4×10^{16} Bq (1 million Ci) of $^{137}Cs^+$ to the vadose zone. The directly measured activity from contaminated sediments has been as high as 10^5 Bq/g (10^7 pCi/g), and indirect field estimates were as high as 10^8 Bq/g (10^{10} pCi/g). Coarse-textured, micaceous sediments that make up the regional surface deposits (*1, 2*) have to a large degree sorbed the $^{137}Cs^+$, limiting vertical migration to distances of approximately 6−20 m (20−65 ft), but in some places $^{137}Cs^+$ has experienced little chemical retardation and has migrated more deeply. The chemical nature and reversibility of the sorption process are uncertain, and concern has focused on whether $^{137}Cs^+$ will migrate over time to groundwater approximately 30−40 m (100−130 ft) below the tanks.

To usefully determine the potential for the future mobilization and transport of $^{137}Cs^+$ in vadose sediments, several unanswered questions must be addressed. First, how strongly is $^{137}Cs^+$ bound to the contaminated sediments? Second, with which mineral components is $^{137}Cs^+$ associated? Third, are there differences in the strength of binding to different mineral components so that the quantity of $^{137}Cs^+$ present in a given location affects mobility? The third question is key. If $^{137}Cs^+$ is abundantly present, it may have saturated highly selective sorption sites and may also be present on low-affinity sites. The latter association would represent $^{137}Cs^+$ that could readily desorb and migrate with the desorbing fluid.

Cs^+ forms no sparingly soluble solid phases that could limit its aqueous concentration (e.g., ref *3*). Retardation of Cs^+ movement in groundwater is therefore controlled by sorption, and Cs^+ is preferentially sorbed by phyllosilicate minerals, which include expansible layer silicates such as smectite and vermiculite and nonexpansible micas such as biotite and muscovite.

The retention of Cs^+ by sediments and phyllosilicates has been intensively studied since anthropogenic $^{137}Cs^+$ became a concern for environmental and health reasons (*4*−*9*). Sorption and desorption were observed to proceed in two steps: rapid initial reaction followed by slower continued reaction (or even renewed sorption, in the case of desorption). This behavior was explained by the hypothetical interaction with three different chemical surface sites: (i) nonselective (fixed charge) exchange sites on phyllosilicate surfaces; (ii) selective frayed edge sites (FES) on micas, formed by the removal of K^+ from the phyllosilicate interlayers; and (iii) interlayer sites in micas, populated by the diffusion of ^{137}Cs from FES. (The transition from weathered vermiculitic 1.4-nm spacing to unweathered 1.0-nm spacing on micas edges—the FES—was hypothesized to form a favorable steric environment for the strong binding of dehydrated cations, e.g., K^+, Cs^+, NH_4^+.) Sorption behavior could be linked to specific exchange sites as follows. Nonselective exchange sites weakly retained $^{137}Cs^+$, which could be readily and rapidly desorbed. The FES sites rapidly and energetically retained Cs^+ and also slowly desorbed Cs^+, depending on system chemistry, explaining the slow sorption/desorption step (*4, 6*). In most experimental studies, complete recovery of sorbed Cs^+ was not achievable, and this unrecovered Cs^+ was considered to be "irreversibly sorbed" or "fixed". Fixed Cs^+ was bound to FES or interlayer sites or both (*6*). More

* Corresponding author e-mail: james.mckinley@pnl.gov; phone: (509)375-6841; fax: (509)375-6954.
† Pacific Northwest National Laboratory.
‡ National Institute for Standards and Technology.

10.1021/es0018116 CCC: $20.00
Published on Web 07/25/2001

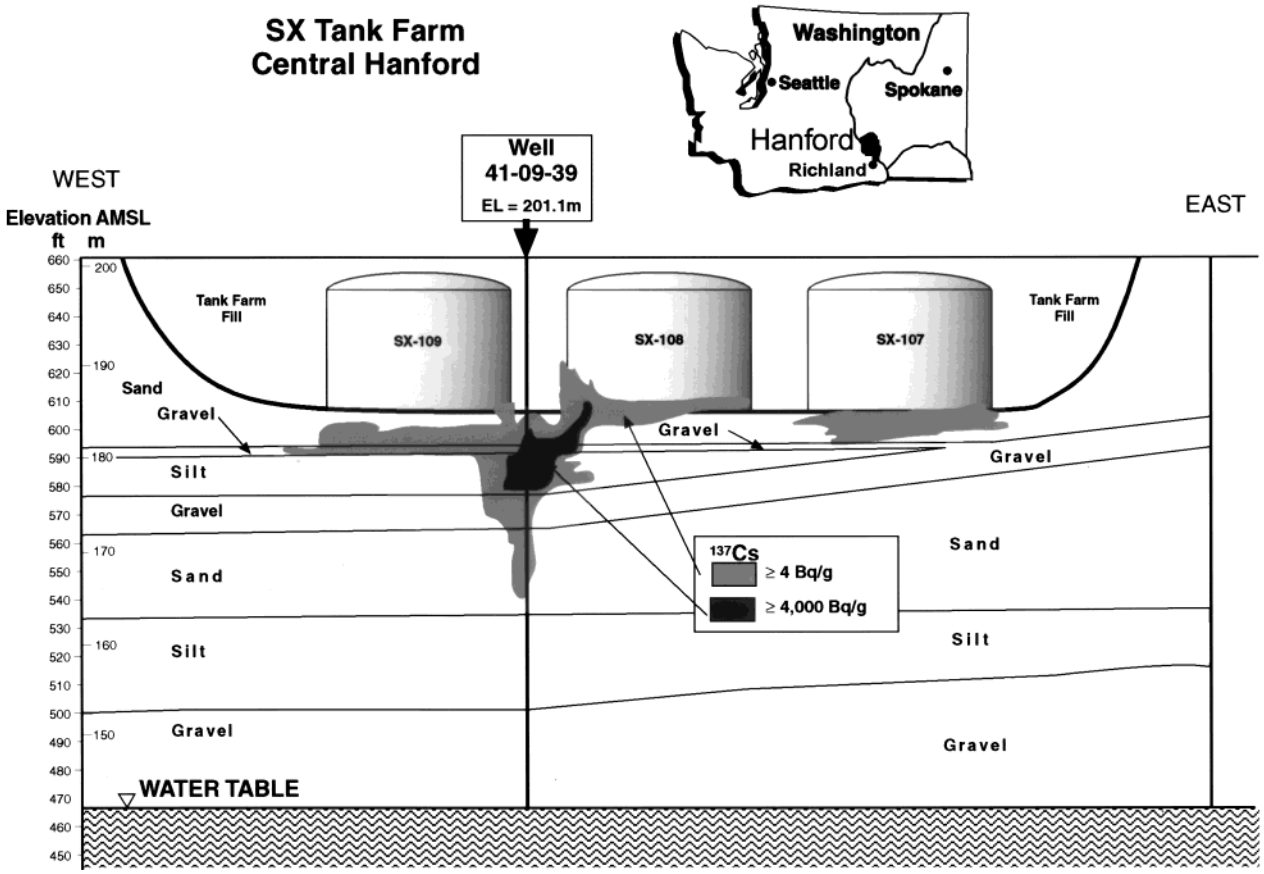

FIGURE 1. Vertical cross section of the SX Tank Farm at Hanford, showing the extent and concentration of ^{137}Cs in contaminated sediments impacted by tank leakage. Well 41-09-39 was constructed to sample the contaminant plume.

recent field data, however, indicated significant desorption of Cs^+, particularly by NH_4^+, over long periods (*5, 10*).

The idea that some Cs^+ was fixed and unrecoverable may be erroneous. The replacement of Cs^+ sorbed to a mineral surface or to interlayer space is controlled by ion-exchange equilibria and is therefore thermodynamically reversible (*4*). The extent of Cs^+ diffusion into interlayer space would probably amount to less than 1 nm/yr (*8*), so it may be that Cs^+ could not penetrate the bulk interlayers at all and was confined to exchange with K^+ on sites at the weathered edge of mica flakes (the FES) (*4*). This suggests that, on the crystal edge, proximal to the transition from 1.0 to 1.4 nm basal spacing, two strong sorption reactions could occur: Cs^+ might bind to sites where K^+ has been removed by weathering, or it might exchange with K^+ that is *just* in interlayer space. To better understand the limits on Cs^+ mobility and its future mobilization potential in Hanford sediments, we examined a restricted set of core samples removed from a ^{137}Cs-contaminated zone beneath a leaky SST and characterized the degree of $^{137}Cs^+$ fixation and its mineral associations.

Materials and Methods

$^{137}Cs^+$ contaminated core samples were obtained from the S-SX Tank Farm at Hanford (Figure 1). The farm contains 30 tanks, including SX-108, which was shown by spectral γ-logging to have leaked and distributed $^{137}Cs^+$ to the vadose zone to a depth of about 37 m (120 ft), with maximum ^{137}Cs activities of $> 4 \times 10^3$ Bq/g (> 100 000 pCi/g). The tank wastes had $[OH]_{tot} > 5$ mol/L and $Al(OH)_4^- > 1$ mol/L. The leak occurred approximately 30 yr ago, ca. 1 half-life for ^{137}Cs. Samples were obtained by cable-tool drilling through the bottom of a dry well (designated 41-09-39) that had been constructed to log the contaminant plume and by coring through the underlying sediments to the water table at a depth of 64.4 m. Continuous cores were removed over the interval from 40 to 49 m, and intermittent samples were collected below that depth. The samples were numbered in sequence with depth and also given arbitrary letter suffixes (Tables 1−3).

TABLE 1. Sieve-Size Results (wt %) for Three Depth Intervals[a]

		depth (m), sample, moisture			
sieve size		40.6, 2C/D, 18.99	40.9, 2A/B, 11.15	41.21, 3A/B, 9.47	46.91, 12A/B, 5.12
	>2 mm	2.15	0.90	0.36	−
very coarse sand	2−1 mm	2.58	0.90	0.97	−
coarse sand	1−0.5 mm	3.48	0.67	1.65	−
medium sand	0.5−0.25 mm	1.92	0.63	0.68	−
fine sand	0.25−0.106 mm	12.77	8.79	8.64	−
very fine sand	0.106−0.053 mm	27.98	37.03	30.62	−
silt and clay	< 0.053 mm	47.91	49.61	56.16	−
total		98.79	97.83	99.07	

[a] Moisture content in wt %. Sediments were wet-sieved, and wt % results (dry wt basis) represent post-sieving fractions of the original bulk sediment. Totals less than 100% represent losses during processing. [b] Values not determined are indicated by −.

The particle size distributions of composite samples were determined using a standard procedure (*11*). Moisture contents were determined gravimetrically. The size distributions of samples, in weight percents, were determined after wet sieving and drying among the size fractions: gravel (>2 mm), very coarse sand (1−2 mm), coarse sand (0.5−1 mm),

TABLE 2. γ-Counting Results for ^{137}Cs (Bq g^{-1}) as a Function of Sediment Size Fractions (dry wt basis)

sieve size		sample 2C/2D	2A/2B	3A/3B	12A/12B
	>2 mm	2301	1909	1006	<1
very coarse sand	2−1 mm	2516	2608	1002	5
coarse sand	1−0.5 mm	1898	2268	821	4
medium sand	0.5−0.25 mm	2671	1391	734	4
fine sand	0.25−0.106 mm	296	45	41	3
very fine sand	0.106−0.053 mm	396	7	21	1
silt and clay	<0.053 mm	584	42	322	10

TABLE 3. Sediment Activities (Bq g^{-1}) Calculated from Tables 1 and 2 and Measured Directly[a]

	2C/2D	2A/2B	3A/3B	12A/12B
measured	1263	48	144	3
calculated	1152	94	225	−

[a] Values not determined are indciated by −.

medium sand (250−500 μm), fine sand (106−250 μm), very fine sand (53−106 μm), and silt plus clay (<53 μm).

Subsamples from each core were placed in containers having precalibrated geometries for γ-energy analysis and were analyzed using 60% efficient intrinsic germanium γ-detectors (Oxford Instruments, Inc.), calibrated against a commercial standard (QCY48A mixed γ; Amersham, Inc). Deadtime was kept below 1%. Data quality was maintained using controls with peaks spanning the full detector range, monitored for peak position, counting rate, and intensity.

Random powder mounts for X-ray diffraction (XRD) were prepared by crushing and were analyzed on a Phillips diffractometer (model 3520) using Co Kα radiation. A separate, oriented clay-mineral mount from the <53-μm fraction was prepared by sedimentation of the <2-μm portion. Operating conditions were 40 keV, 40 mA for the anode, with the goniometer scanning at 2 s/0.05° 2θ step from 5° to 75° 2θ.

We conducted experiments to determine whether the desorbable quantity of $^{137}Cs^+$ could be increased by chemical pretreatment to remove secondary minerals that could "armor" sorption sites. In each case, 1.5 g of sediment was reacted with the pretreating reagent, and the slurry was centrifuged, decanted, and washed with 20 mL of deionized water by shaking for 2 h and then centrifuged and decanted again. The wet sediment was reserved for desorption experiments. The reactant solution and wash water were radiocounted. ICP-MS measurements of Fe^{2+} were made to calculate the amounts removed per gram of reacted sediment. A parallel procedure was done in which 5 g of sediment was treated, washed, and radiocounted for mass balance calculations.

Four chemical treatments were used to target different sediment qualities that could affect the sorption and retention of $^{137}Cs^+$. (i) Sodium dithionite was used to remove total free iron oxide (*12*). Sediment was reacted with 40 mL of 0.3 M sodium citrate and slowly heated to 80 °C in a water bath, then 0.5 g of sodium dithionite was added, and the mixture was stirred for 5 min. A second 0.5 g of sodium dithionite was added, and the mixture was stirred for 10 min. (ii) Tamm's reagent was used to remove amorphous iron oxide (*12*). Sediment and 30 mL of 1 M ammonium acetate, adjusted to pH 5.5, were added to separate 50-mL centrifuge tubes. After the solution was mixed for 1 h, the pH was adjusted to 5.5; the tubes were centrifuged and decanted; and 30 mL of 0.175 M ammonium oxalate/0.1 M oxalic acid solution, adjusted to pH 3.0, was added. The centrifuge tubes were wrapped with aluminum foil and shaken for 2 h. (iii) Potassium hydroxide was used to remove amorphous aluminum oxides (*13*). Sediment was mixed with 10 mL of 4 M potassium hydroxide and shaken for 10 min, and 100 mL of deionized water and 5 drops of 0.5% phenolphthalein were added to each flask. A total of 4 M HCl was added until each solution was colorless. (iv) Nitric acid was used as a harsh extractant/desorber. Sediment was reacted with 10 mL of 2 M nitric acid and stirred for 24 h.

Rubidium (0.1 M $RbNO_3$), for which micas have an affinity similar to that for Cs^+ (*14, 15*), was used to induce desorption. (Since nitric acid is a strong desorber, the samples treated with nitric acid were not extracted with Rb^+.) The wet equivalent of 0.40 g dry weight of sediment was transferred to centrifuge tubes, in triplicate, and suspended in 50 mL of 0.1 M $RbNO_3$ solution. The tubes were shaken in duplicate sets for 1 and 29 days and then centrifuged, and the supernatant was counted for ^{137}Cs.

Autoradiography, used previously in environmental studies of radioactive particles (*16, 17*), was used to identify $^{137}Cs^+$-containing mineral particles and to quantify their activity levels. The particles were disseminated onto glass slides and exposed for 4320 min using a 20 cm × 25 cm Fujifilm BAS-TR 2025 phosphor-plate, which was scanned with a Fuji BAS-5000 digital autoradiography instrument at a 25-μm pixel setting. The distribution of radioactivity on each was imaged, and grains were designated as "positive" or "negative" based on their ability to generate a radioactivity spot on the image. Secondary slides of segregated positive and negative grains were again imaged to confirm that grains of each designation were correctly identified. In addition, micas identified as biotite, vermiculite, or muscovite from the 56−105- and 105−250-μm size fractions were affixed to slides in sets of six each (36 flakes total) for autoradiographic analysis without prior screening, and 24 micas were mounted (one per slide) for quantitative analysis. For quantitation, the pixel intensities associated with each grain were integrated. Background radiation intensities were measured from blank slides, and the mean of the background was subtracted from each grain area value to yield a background-subtracted intensity for each grain. This value was expressed in photostimulated luminescence (PSL) units, characteristic for this technique, which is linear with dose rate (*18, 19*). Uncertainties were evaluated using the standard deviation of the mean of the background counts (*20*). γ-Spectrometry results (methods described below) were regressed against the bulk phosphor measurements, producing an indirect calibration curve (*21*). The linear regression between the activity and PSL units (valid over several orders of magnitude of activity) was used to estimate the activity of particles that had not been counted by γ-spectrometry, within the uncertainty determined by the regression.

The separated particles were individually assayed for $^{137}Cs^+$ with a low-background γ-ray spectrometer (*22*) nominally for 24 h. The efficiency was calibrated for this geometry against a point-source Standard Reference Material (SRM 4215B). A 10-day background measurement with a blank slide showed no detectable ^{137}Cs. Potassium-40 in the slides

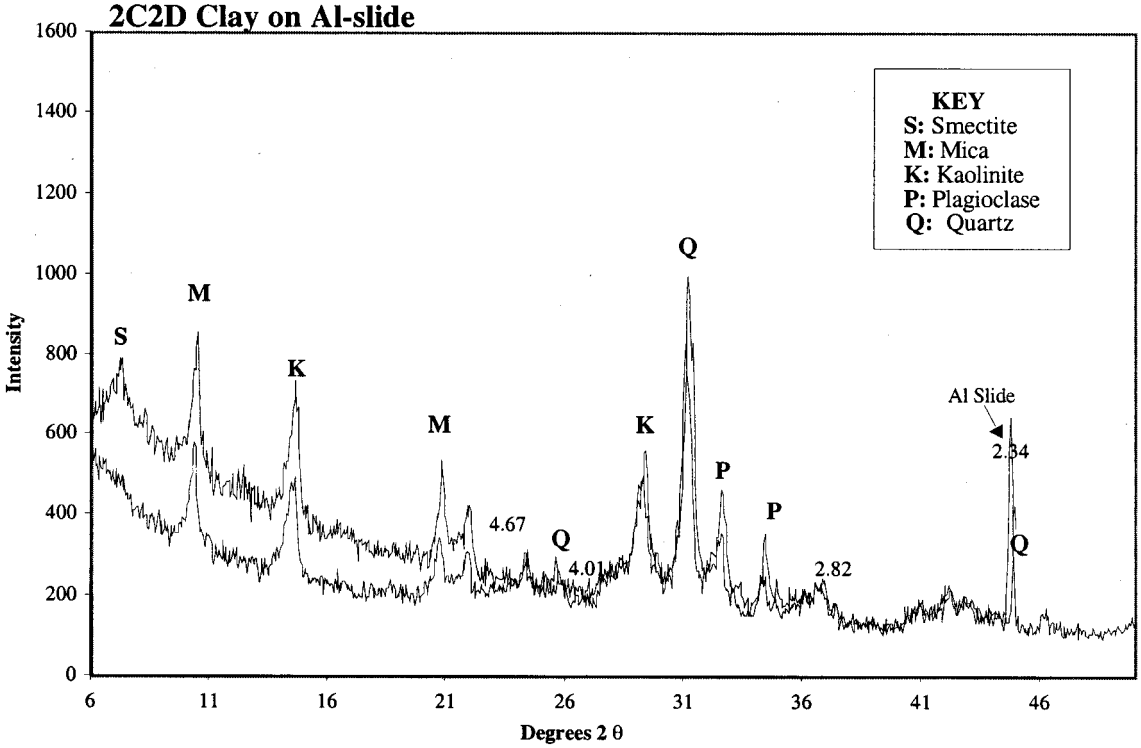

FIGURE 2. X-ray diffraction results from the clay-sized fraction (<2 μm) of sample 2C/D from well 41-09-39. Upper line, Mg saturated; lower line, ethylene glycol saturated.

was monitored as a measure of the system's stability; the potassium counting rate was the same for all samples within statistics. The ^{137}Cs region of the spectrum was integrated with a fixed-boundary algorithm (*23*). Error estimates were computed according to standard methods (*24*).

For phase identification, samples were examined optically using a CCD-equipped Leitz 2000 petrographic microscope and a JEOL JXA-8600 electron microprobe. Optical images were used as maps to examine the qualitative elemental compositions of individual grains, and the compositional information obtained by energy dispersive spectrometry was combined with noted optical properties to identify common rock-forming minerals. For example, a dark grain with distinct platy morphology including Fe and K was unambiguously biotite, and an equant grain composed of Si and O was identified as quartz. In the case of ^{137}Cs-bearing grains, mineral composites were dissected during optical examination.

Results and Discussion

Sediment Characterization. For detailed study, we focused on samples from depths of 40.60−41.21 m (133−135 ft). Bulk-sediment γ-counting (Table 3) showed that this interval had markedly elevated radioactivity relative to deeper, apparently less contaminated sediments. The uppermost sample (2C/D) contained the most ^{137}Cs (activity of 1263 Bq g^{-1}), and ^{137}Cs activity differed by a factor of over 400 between contaminated and uncontaminated sediments.

Fractional size analysis by sieving (Table 1), showed the sediments to consist predominantly (more than 75% of the total mass) of materials less than 106 μm in diameter. Moisture contents decreased from ca. 20 wt % in 2C/D to ca. 5 wt. % in 12A/B. Water used during drilling through the original base of the well casing may have contributed to elevated moisture in the upper samples; 5 wt % moisture is typical of Hanford vadose sediments (*25*). Examination of the subsamples revealed that some sediment clasts had aggregated into fragments composed of clay-sized and larger material and that fragments could be larger than the largest size passable through the overlying sieve. Individual mineral components of these aggregates, however, were smaller than the allowable upper diameter: large clasts did not pass through small sieve openings. Also, clay-size material was present in larger fractions (>53 μm) because rinsing during sieving did not remove all silt and clay-sized material.

After sieving and drying, individual size fractions were counted for ^{137}Cs activity (Table 2). For comparison with the bulk measurements (Table 3), the total activity of each sediment was calculated from the weight percent and size-fraction activity values. For sample 2C/D, the calculated value was within 10% of the bulk value; for sample 2A/B, where the bulk activity was much lower, ca. 4% of the activity for 2C/D, the agreement was within a factor of 2. In the upper sediments (2C/D, 2A/B, and 3A/B), the coarser fractions had the highest ^{137}Cs activity per unit mass. The relationship between grain size and mass-normalized activity suggested that the coarser fractions could contain a large portion of the sorbed ^{137}Cs, but because the coarser sizes constituted only a minor mass fraction of the sediments, the largest part of the total ^{137}Cs activity was contained in the silt and clay material.

Optical examination of the sediments showed discrete, large mica flakes in the coarser sediments (0.25 mm and larger). In finer sediments, micas were present individually and as a component of aggregates. The micas could be operationally identified based on texture and color as biotite (black), muscovite (clear and most abundant), and vermiculite (rust and least abundant). XRD of individual sieve sizes (data not shown) indicated the presence only of quartz, plagioclase, and mica (undifferentiated) in all size fractions. Analysis of the clay-size fraction (Figure 2) indicated the presence of kaolinite, quartz, plagioclase, smectite, and mica fragments.

The activity measurements and petrographic observations were consistent with the preferential binding of ^{137}Cs^{+} by nonexpansible phyllosilicates, particularly micas (*7, 9, 26*). Since Cs^{+} is less selectively bound by smectite and kaolinite,

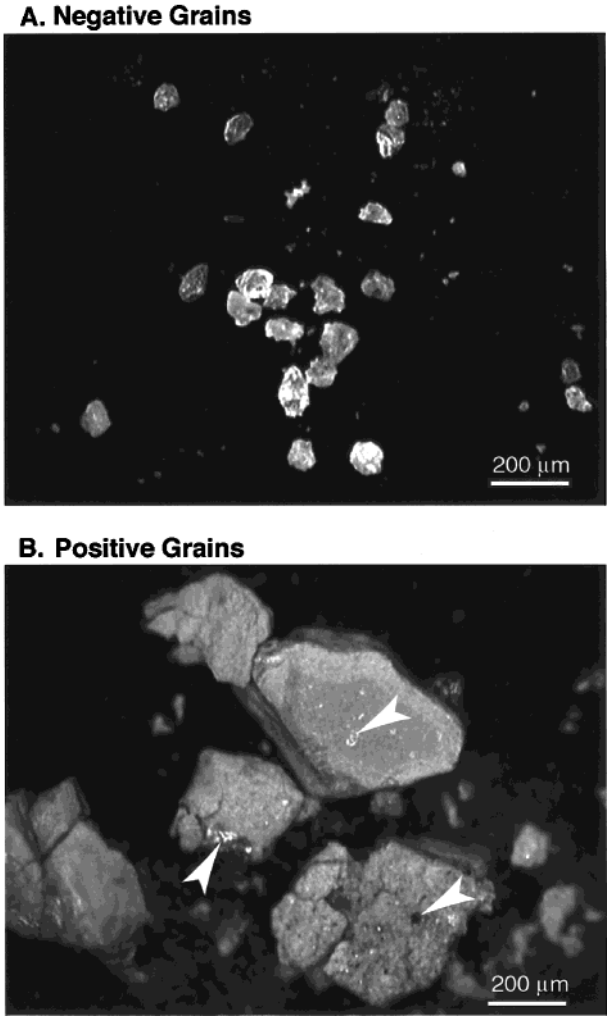

FIGURE 3. Photomicrographs of representative grains from the 53−106-μm sieved fraction. (A) Negative grains and (B) positive grains are aggregates of smectite and silicate minerals, apparently flocked during sieving. Arrows indicate micas.

relatively small quantities of nonexpansible phyllosilicates could predominate in determining sediment $^{137}Cs^+$ activities. In separate research (*27*), the sorption and desorption of Cs^+ on uncontaminated sediments from this stratum were described by a multisite model including a high-affinity site analogous to FES on micas. The coarse fraction (>0.25 mm) contained abundant large flakes of mica, along with primary silicates, such as quartz and feldspar. The latter would not be expected to significantly sorb $^{137}Cs^+$. The intermediate fractions (0.053−0.106 mm) consistently showed lower unit-mass activities than the bracketing coarse and fine sizes (>0.25 and <0.053 mm; Tables 1−3). The inclusion of relatively less of the micaceous component and of little silt-clay component in these intermediate size ranges could explain their relatively low unit-mass activities. Micas may have mechanically weathered from relatively large flakes to produce <53-μm fragments, but few flakes of intermediate size. This explanation is admittedly ad hoc but is consistent with the observations. In the fine fraction (<0.053 mm), expansible phyllosilicates were abundant, and these were expected to contribute high concentrations of low-affinity sites for $^{137}Cs^+$ adsorption. Micaceous minerals were ubiquitous components of this fraction also, and the unit-mass activity of ^{137}Cs for the <0.053-mm size fraction could have a significant contribution from mica-bound $^{137}Cs^+$. The size-fraction activity results are thus consistent with the selective binding of Cs^+ by nonexpansible phyllosilicates.

TABLE 4. Single-Grain Radioactivity Counting Results

size (μm)	no.	PSL/min[a]	Bq[b]	Bq SD[a]
500−250	101	0.027	−[c]	−
	102	0.014	0.018	0.005
	103	−	0.009	0.005
	104	0.035	0.064	0.006
	105	0.010	0.010	0.005
	106	0.016	0.014	0.005
250−106	101	0.036	0.044	0.005
	102	−	−0.008	
	103	0.005	−0.012	
	104	0.014	−	
	105	0.0037	0.007	0.005
	106	0.016	0.007	0.005
106−53	101	0.021	0.014	0.005
	102	0.012	0.016	0.005
	103	0.026	0.032	0.006
	104	0.041	0.047	0.006
	105	0.024	0.020	0.005
	106	0.040	−	

[a] PSL units are based on background subtracted integrated areas after 4320 min (3 d) of exposure. Background intensities were 0.0324 ± 0.0005 PSL min^{-1} (21 measurements). [b] Bq measurements are by low-level γ-counting with counting uncertainties at the 1σ level. A measurement of activity against SRM 4215B gave 2065 Bq ± 8. [c] Unmeasured quantities are indicated by −.

Radiological Screening and Analysis. The research consensus has been that the small fraction of highest energy sites on the frayed edges of micas most strongly retain Cs^+. Numerous investigations have shown the micaceous sheet silicates to be important in cesium immobilization; however, the experiments using specimen substrates were not field-based, and field investigations have been hampered by the very small activities (below the detection limit) of $^{137}Cs^+$ present on the surface of individual mineral grains. The strong adsorption of Cs^+ by illite has been demonstrated experimentally (*6, 8, 14, 28, 29*), and, thus micaceous minerals were inferred to be responsible for the retention of $^{137}Cs^+$ in sediments where a fraction of the total $^{137}Cs^+$ could not be desorbed (*5, 30*). Francis and Brinkley (*31*) used a density separation method to show the presence of mica at low concentration in a contaminated sediment and found that the mica-including density fractions were enriched in ^{137}Cs, deductively demonstrating that micas were an important $^{137}Cs^+$-retaining phase. Our results confirm directly the importance of micas in binding $^{137}Cs^+$ in contaminated sediments.

Digital phosphor-plate images provided a means of rapid detection and identification of $^{137}Cs^+$-sorbing particles. Sediment clasts that showed positive autoradiography results were morphologically and mineralogically distinct from negative clasts. In the fine and very fine sand fractions (53−250 μm), the positive clasts consisted of mineral fragments bound together by clay. As shown in Figure 3a, for the 53−106-μm fraction, the negative clasts were predominantly particles of quartz and plagioclase feldspar, with some surface staining by fine iron oxide. The positive clasts, in contrast, were consistently larger than the maximum size nominally allowed by the sieving procedure: they were aggregates (Figure 3b). Close examination of the aggregates showed an abundance of mica. The grains in Figure 3b have partially disaggregated during manipulation, revealing micas as either translucent large flakes or as small, dark constituent flakes at the surface of the clumped material. Examination of disaggregated positive grains using optical and electron microscopy showed them to consist of quartz and plagioclase as well as mica and smectite.

The single-grain exposure measurements from autoradiography images provided a numerical value for radioactivity

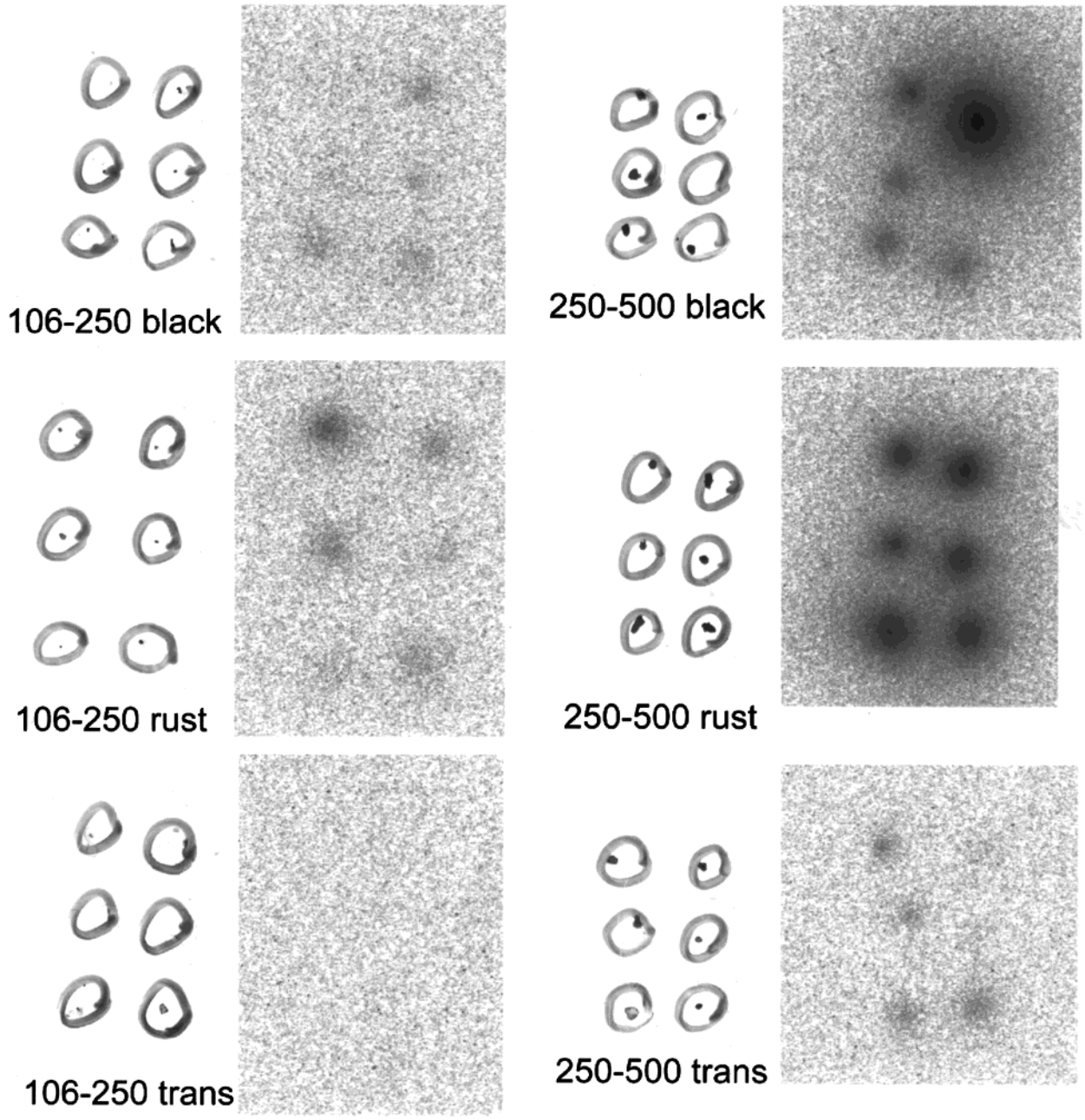

FIGURE 4. Digital autoradiographs and optical micrographs of mica flakes hand-picked from contaminated sediments. Size fractions are indicated in micrometers (e.g., 106−250 μm). Mica phases were differentiated by color: black, biotite; rust, vermiculite; and trans(parent), muscovite. Each mica was mounted to the glass slide and circled on the underside using a marking pen.

(in units of PSL). These numerical results had good correspondence to γ-counting measurements ($r^2 = 0.83$). PSL signals may have originated from ^{137}Cs β- or γ-radiation or both (*32*). γ-Counting at the appropriate energy confirmed ^{137}Cs as the radiation source. PSL measurements were more sensitive than γ-counting and thus could estimate ^{137}Cs activities that were detectable by the phosphor system when these same activity levels were too small to be detected by γ-spectrometry. This was utilized for particle 250-103 and improved the confidence in the uncertain γ-detection of particles 250-106 and 250-105 (Table 4).

The examination of positive clasts suggested that the selection of clasts for single-clast autoradiography and γ-counting might be biased toward agglomerated small particles, since the strongest radiological results would tend to come from relatively large aggregates of materials including numerous positive components. We determined the relative significance of different agglomerate components by logically evaluating the autoradiography results and by performing additional autoradiography measurements. The primary silicates (quartz and feldspar), incorporated in the agglomerates, could be ruled out as sources of radiation by analogy to negative clasts. The retention of $^{137}Cs^+$ by micas was tested directly by picking mica flakes from the 0.106−0.250- and 0.250−0.500-mm size fractions (Figure 4). The micas were all confirmed to significantly retain $^{137}Cs^+$ by producing positive autoradiographs. Biotite and vermiculite showed strongly positive results, with muscovite retaining less $^{137}Cs^+$ than the other micas. During physical manipulation, "vermiculite" flakes often delaminated and were observed to consist of a rusty cover or sheath of vermiculite over a relatively pristine core of biotite; the retention of $^{137}Cs^+$ ascribed to vermiculite was therefore likely due to retention by biotite or a composite of biotite and vermiculite. The three micas in any case showed a higher affinity than other phases for $^{137}Cs^+$. In coarser fractions, only micaceous minerals were

TABLE 5. Chemical Treatment and Desorption Results for Size Fractions of Sample 2C/D[a]

		chemical treatment results (mean of duplicate)			Rb desorption results (triplicate) % ^{137}Cs removed			
treatment	sample (μm)	Fe dissolved[b]	sediment dissolved[b]	% ^{137}Cs removed	1 d mean	1σ	29 d mean	1σ
dithionite	bulk	1.3	5	5.6	6	2	14	2
	250−106	–	–	7.8	6	3	20	2
	<53	0.80	7	5.2	10	2	21	4
Tamm's	bulk	0.44	3	5.3	3	1	8	0
	250−106	–	–	7.5	7	1	22	4
	<53	0.66	6	5.0	8	1	19	5
KOH	bulk	bd	1	1.8	4	1	10	1
	250−106	bd	–	2.3	13	7	22	1
	<53	bd	2	2.3	4	2	14	1
HNO_3	bulk	2.3	9	23.3	–		–	
	250−106	–	–	16.7	–		–	
	<53	1.0	26	16.0	–		–	
untreated	bulk	–	–	–	3	1	5	2

[a] ^{137}Cs activities by γ-counting. All values in %. –, no data; bd, below detection limit. The wt % Fe in the original sediments were <53 μm, 4.82; bulk sediment, 3.32. The % ^{137}Cs removed is relative to values in Table 1. [b] Wt % of sediment.

present to sorb $^{137}Cs^+$. In finer fractions, smectite was also present and could sorb $^{137}Cs^+$, but the waste solutions that bore $^{137}Cs^+$ were high in Na^+, which suppresses Cs^+ adsorption to low-affinity sites on smectites. The other mineral phases, primary silicates, do not significantly retain Cs^+. The observation that coarse fractions sorb $^{137}Cs^+$ disproportionate to their abundance and the presence of micaceous minerals in those fractions as the only $^{137}Cs^+$-retaining phase, suggested that micas are the predominant control of Cs^+ mobility in these sediments.

Chemical Treatment and Desorption Experiments. The $^{137}Cs^+$-containing waste solutions were hot and contained high base (OH^-) and aluminate [$Al(OH)_4^-$], which may have induced the dissolution of phyllosilicates containing oxidizable Fe(II) and the precipitation of secondary phases including ferric oxyhydroxides and aluminum oxide. Our dissolution/desorption experiments suggested that secondary phases affected the desorption of $^{137}Cs^+$ (Table 5). The untreated bulk sediment released only 5% of the total sorbed $^{137}Cs^+$ when reacted with Rb^+ for 29 days (Table 5). The use of chemical pretreatments increased the release of sorbed $^{137}Cs^+$. The precipitation of secondary phases, either directly from waste solutions or after reaction with the sediment, may have blocked surface sorption sites, which were accessible to Rb^+ after their dissolution. Since nitric acid could both dissolve secondary phases and desorb $^{137}Cs^+$ by exchange with H^+, treatment with nitric acid alone was equivalent in some ways to dissolution/desorption. Nitric acid dissolved a significant percentage of the reacted sediment and removed $^{137}Cs^+$ that approximately equaled the amount removed by the other treatments. Pretreatment with iron-extracting (dithionite and Tamm's) and aluminum-extracting (KOH) solutions caused a marked increase in $^{137}Cs^+$ desorption to 15−30% of the total. In the three pretreatments, the fractions of $^{137}Cs^+$ removed by exchange with Rb^+ for 29 days were approximately equivalent. These results were consistent with the formation of an armor of secondary precipitates of iron or aluminum oxide on the surfaces of sorbing solids that prevented exchange of $^{137}Cs^+$ with the aqueous phase; $^{137}Cs^+$ desorption from interlaminar wedge or planar sites on the sorbing phyllosilicates followed the dissolution of these phases by pretreatment.

An alternative explanation is suggested by the extent of $^{137}Cs^+$ extraction prior to desorption, and other extraction data included in Table 5. Data are few, i.e., four points, but within a given size fraction there is a strong correlation between the fraction of sediment dissolved and the $^{137}Cs^+$ removed during chemical treatment (the correlation of wt % sediment dissolved to % $^{137}Cs^+$ removed was $r^2 = 0.88$ for bulk sediment and $r^2 = 1.00$ for the <53-μm fraction). The $^{137}Cs^+$ may have been removed from FES by reaction dissolution of the mica edges with the pretreatment agents. The $^{137}Cs^+$ freed by dissolution (or by desorption by the K or NH_4^+ component of the pretreatment) would then have resorbed to available surface sites. Desorption with Rb^+ immediately following extraction could then have removed the resorbed $^{137}Cs^+$, contributing to the apparent large increase in desorbable $^{137}Cs^+$ seen in Table 5. The $^{137}Cs^+$ liberated to solution by pretreatment would only have been sorbed for a short period before desorption with Rb^+. Although binding of Cs^+ to surface sites on micas may be strong and selective, desorption soon after binding is more effective than desorption after the passage of time (*5, 6*). The time dependence of $^{137}Cs^+$ desorption over 1−29 days may thus result from the inverse of slow-binding kinetics for fixation to selective sites (*8*). This explanation is supported indirectly by dissolution data (Table 5); while the amount of iron dissolved by iron-extracting reagents amounted to about one-half to a little more than 1 wt %, the percent of bulk sediment dissolved was 3−7 wt %. Reaction with KOH dissolved 1−2 wt % of the sediment. Either type of reagent (iron-reducing or alumina-dissolving) could have attacked the weathered FES on iron-bearing silicates, destroying them and removing the $^{137}Cs^+$ bound to them. The FES were present in gross overabundance to $^{137}Cs^+$ and also could have been recreated at chemically reacted mineral surfaces, providing sites for the readsorption of liberated $^{137}Cs^+$.

At most, less than 30% of the available $^{137}Cs^+$ was removed by pretreatment and desorption with Rb^+. $^{137}Cs^+$ in contact with FES for 30 yr may have participated in ongoing exchange with interlayer K^+, and these sites may have been less reacted than FES during pretreatment. Also, only a fraction of the $^{137}Cs^+$-binding FES may have been altered by pretreatment solutions, leaving a significant fraction of the sorbed $^{137}Cs^+$ on mineral surfaces.

Long-Term Retention of Cs. The combination of sediment characterization with the chemical treatment and subsequent desorption of $^{137}Cs^+$ provides data that can be integrated to provide information on the retention of Cs leaked from HLW waste-storage tanks.

The chemical leaching of sediments by chemical reagents suggested that some iron oxide minerals were present. Dithionite and Tamm's reagent removed 28 and 9% of the sediment total iron, respectively (Table 5), whereas treatment

of the bulk sample with nitric acid removed 48% of the total Fe. The presence of iron oxyhydroxides does not suggest that they contributed to ^{137}Cs immobilization. It is unlikely that the adsorption of $^{137}Cs^+$ to iron (or aluminum) oxides contributed to immobilization since Cs^+ is weakly and nonspecifically sorbed by oxides of Fe, Mn, and Al (*33*−*38*). Excess concentrations of other monovalent cations (e.g., Na^+) virtually eliminate Cs^+ adsorption to metal oxides through competitive mass action (*39*).

The silicate minerals other than the phyllosilicates can be dismissed as significant contributors to Cs^+ retention. While the surfaces of grains of the primary silicates (quartz, feldspar, etc.) can be conceptualized to possess chemically altered surfaces capable of sorbing Cs^+ (e.g., smectite-like surfaces), our data do not identify any significant sorption of ^{137}Cs to silicate clasts. All positive digital autoradiography images were associated with clasts containing mica, and all negative clasts were primary silicates (quartz and feldspar).

The remaining ^{137}Cs-associated phases were either specifically identified to be micas or were multi-mineral clasts including micas and expansible layer silicates. The XRD analysis of the clay-sized fraction included kaolinite, smectite, plagioclase, and quartz along with mica.

The potentially significant sorbers for Cs^+ fall into two components with differing properties: strongly sorbing nonexpansible phyllosilicates (micas) with relatively low cation-exchange capacity (CEC) and more weakly sorbing expansible phyllosilicate clay minerals with relatively high CEC. Cesium has been widely observed to be strongly and selectively adsorbed by micaceous minerals in soils and sediments (*7, 26, 29, 31*). It is also readily adsorbed by other phyllosilicates where its behavior is similar to other cations (*15*) and less selectively and strongly bound than on micas. The sediment system may thus be considered to consist functionally of a set of strong and weak binding sites with the strong sites preferentially binding Cs^+ until they are at or near saturation, followed by Cs^+ binding to weaker sites. These observations have been made for other mineral and sediment systems (*5, 9*) and have led to the application of multisite models to describe Cs^+ sorption (*40*−*43*).

In sediments contaminated 30 yr ago with tank-derived HLW, the majority of $^{137}Cs^+$ was apparently strongly bound to FES. Our extraction and desorption results suggested that approximately 70−80% of the sorbed $^{137}Cs^+$ (i.e., the fraction not exchangeable with Rb^+) was bound by these sites and does not present much concern for future mobilization by less reactive fluids. Some of the sorbed $^{137}Cs^+$ in the contaminated sediments may have been bound to phyllosilicate clay minerals. The quantity of $^{137}Cs^+$ sorbed to expansible phyllosilicate clays could be readily mobilized by exchange with other cations and could migrate with desorbing solutions. Careful experimental evaluation of the partitioning of $^{137}Cs^+$ to micas and clays and of the potential effects of high concentrations of competing cations must be completed before conclusions are drawn regarding the mobility of desorbable $^{137}Cs^+$. However, uncontaminated micas downgradient from the point of desorption in vadose subsurface sediments would strongly retard future $^{137}Cs^+$ migration, limiting potential breakthrough to groundwater.

The ultimate $^{137}Cs^+$ concentration in these sediments was very low (ca. 1.0×10^{-11} mol/g). In a related paper (*27*), we have comprehensively studied Cs^+ adsorption to a pristine analogue of the contaminated material studied here. Through a multisite modeling approach, we estimated that the total concentration of high-affinity FES sites in the bulk sediment was quite low (e.g., 3.45×10^{-8} mol equiv/g or 0.08% of the total CEC). Despite the paucity of high-energy sites, the total $^{137}Cs^+$ in the contaminated sediment could be bound by only 0.008% of them. Even if the total Cs^+ concentration was taken to be about five times the $^{137}Cs^+$ concentration ($^{137}Cs^+$ was ca. 20% of the total Cs^+ extracted after cation exchange for 31 days; data not shown), the total exchangeable Cs^+ would amount to a tiny fraction of the high-energy sites. Thus, the high-energy sites on micas are abundant, and partitioning to the expansible phyllosilicates seems unlikely.

Acknowledgments

We would like to thank two anonymous reviewers whose detailed comprehensive comments greatly improved the manuscript. This work was supported in part by the U.S. Department of Energy, Office of Science and Office of Environmental Management, Environmental Management Science Program. Pacific Northwest National Laboratory is operated by Battelle Memorial Institute for the U.S. Department of Energy. Certain commercial equipment, instruments, or materials are identified to specify experimental procedures. Such identification does not imply recommendation or endorsement by the National Institute of Standards and Technology or the Pacific Northwest National Laboratory.

Literature Cited

(1) Tallman, A. M.; Fecht, K. R.; Marratt, M. C.; Last, G. V. *Geology of the Separations Areas, Hanford Site, South-Central Washington*; Report RHO-ST-23; Rockwell Hanford Operations: Richland, WA, 1979.
(2) Freeman-Pollard, J. R.; Caggiano, J. A.; Trent, S. J. *Engineering Evaluation of the GAO/RCED-89-157, Tank 241-T-106 Vadose Zone Investigation*; Report BHI-00061; Bechtel Hanford, Inc.: Richland, WA, 1994.
(3) Parkhurst, D. L.; Appelo, C. A. J. *User's Guide to PHREEQC (Version 2)—A computer Program for Speciation, Batch-Reaction, One-Dimensional Trahsport, and Inverse Geochemical Calculations*; U.S. Geological Survey: Denver, CO, 1999.
(4) Cornell, R. M. *J. Radioanal. Nucl. Chem.* **1993**, *171*, 483.
(5) Evans, D. W.; Alberts, J. J.; Roy A.; I. C. *Geochim. Cosmochim. Acta* **1983**, *47*, 1041.
(6) Comans, R. N. J.; Hockley, D. E. *Geochim. Cosmochim. Acta* **1992**, *56*, 1157.
(7) Sawhney, B. L. *Clays Clay Miner.* **1970**, *18*, 47.
(8) Comans, R. N. J.; Haller, M.; de Ptreter, P. *Geochim. Cosmochim. Acta* **1991**, *55*, 433.
(9) Francis, C. W.; Brinkley, F. S. *Nature* **1976**, *260*, 511.
(10) Smith, J. T.; Comans, R. N. J.*Geochim. Cosmochim. Acta* **1996**, *60*, 995.
(11) ASTM. *Method D422-63*; American Society for Testing and Materials: West Conshohoken, PA, 1998.
(12) Loeppert, R. H.; Inskeep, W. P. In *Methods of Soil Analysis, Part 3. Chemical Methods*; Sparks, D. L., Ed.; Soil Science Society of America: Madison, WI, 1996.
(13) Holmgren, G. G.; Kimble, J. M. *Soil Sci. Soc. Am. J.* **1984**, *48*, 1378.
(14) Brouwer, E.; Baeyens, B.; Cremers, A. *J. Phys. Chem.* **1983**, *87*, 1213.
(15) Sposito, G. *The Chemistry of Soils*; Oxford University Press: New York, 1989.
(16) Betti, M.; Tamborini, G.; Koch, L. *Anal. Chem.* **1999**, *71*, 2616.
(17) Saari, H.; Luokkanen, S.; Kulmala, M.; Lehtinen, S.; Raunemaa, T. *Health Phys.* **1989**, *57*, 975.
(18) Zeissler, C. J.; Wight, S. A.; Lindstrom, R. M. *Appl. Radiat. Isot.* **1998**, *49*, 9.
(19) Zeissler, C. J.; Lindstrom, R. M.; McKinley, J. P. *J. Radioanal. Nuclear Chem.* **2001**, *48*, 407.
(20) Taylor, B. N.; Kuyatt, C. E. *Guidelines for Evaluating and Expressing the Uncertainty of NIST Measurement Results*; NIST Technical Note 1297; National Institute of Standards and Technology: Gaithersberg, MD, 1993.
(21) Miyahara, J. *Chem. Today* (*Tokyo*) **1989**, *223*, 29.
(22) Lindstrom, R. M.; Lindstrom, D. J.; Slaback, L. A.; Langland, J. K.; *Nuclear Instrum. Methods Phys. Res.* **1990**, *A299*, 425.
(23) Lindstrom, R. M. *Biol. Trace Element Res.* **1994**, *43*−*45*, 597.
(24) Currie, L. A. *Anal. Chem.* **1968**, *40*, 586.
(25) McKinley, J.; Zachara, J. M.; Fredrickson, J. K.; Stevens, T. O.; Kieft, T. L.; Balkwill, D. L.; Ghiorse, W. C.; Rawson, S. A.; Long, P. E. *Proceedings of the 2nd International Symposium on Subsurface Microbiology*, Bath, U.K., 1993.
(26) Sawhney, B. L. *Clays Clay Miner.* **1972**, *20*, 93.
(27) Zachara, J. M.; Smith, S. C.; Serne, R. J.; McKinley, J. P.; Gassman, P. *Geochim. Cosmochim. Acta*, in press.

(28) Poinssot, C.; Baeyens, B.; Bradbury, M. H. *Geochim. Cosmochim. Acta* **1999**, *63*, 3217.
(29) Tamura, T.; Jacobs, D. G. *Health Phys.* **1960**, *2*, 391.
(30) Grutter, A.; Gunten, H. R. v.; Rossler, E.; Keil, R. *Radiochim. Acta* **1994**, *64*, 247.
(31) Francis, C. W.; Brinkley, F. S. *Nature* **1976**, *260*, 511.
(32) Lederer, C. M.; Shirley, V. S.; Browne, E.; Dairiki, J. M.; Doebler, R. E.; Shihab-Elden, A. A.; Jardine, L. J.; Tuli, J. K.; Buyrn, A. B. *Table of Isotopes*, 7th ed.; John Wiley & Sons: New York, 1978.
(33) Helferrich, F. *Ion Exchange*; McGraw-Hill Book Co.: New York, 1962.
(34) Tien, H. T. *J. Phys. Chem.* **1965**, *69*, 350.
(35) Churms, S. C. *J. S. Afr. Chem. Inst.* **1966**, *19*, 98.
(36) Abendroth, R. P. *J. Colloid Interface Sci.* **1970**, *34*, 591.
(37) Breuwsma, A.; Lyklema, J. *Discuss. Faraday Soc.* **1971**, *52*, 324.
(38) Venkataramani, B.; Venkateswarlu, K. S.; Shankar, J. *J. Colloid Interface Sci.* **1978**, *67*, 187.
(39) Kinniburgh, D. G.; Jackson, M. L. In *Adsorption of Inorganics at Solid−Liquid Interfaces*; Anderson, M. A., Rubin, A. J., Eds.; Ann Arbor Science Publishers: Ann Arbor, MI, 1981.
(40) Wauters, J.; Elsen, A.; Cremers, A.; Konoplev, A. V.; Bulgakov, A. A.; Comans, R. N. J. *Appl. Geochem.* **1996**, *11*, 589.
(41) Wauters, J.; Vidal, M.; Elsen, A.; Cremers, A. *Appl. Geochem.* **1996**, *11*, 595.
(42) Wauters, J.; Elsen, A.; Cremers, A. *Appl. Geochem.* **1996**, *11*, 601.
(43) De Preter, P.; Van Loon, L.; Maes, A.; Cremers, A. *Radiochim. Acta* **1991**, *52/53*, 299.

Received for review October 26, 2000. Revised manuscript received May 15, 2001. Accepted May 22, 2001.

ES0018116